

1
2
3 **Phase separation in fungi**

4
5
6 **Mae I. Staples^{1#}, Corey Frazer^{1#}, Nicolas L. Fawzi² and Richard J. Bennett^{1*}**

7
8
9 ¹Department of Molecular Microbiology and Immunology,

10 ²Department of Molecular Biology, Cell Biology and Biochemistry,
11 Brown University, Providence, RI 02912

12 [#]These authors contributed equally

13 *Correspondence: Richard_Bennett@brown.edu

15 **Abstract**

16 **Phase separation, in which macromolecules partition into a concentrated phase that is**
17 **immiscible with a dilute phase, is involved with fundamental cellular processes across the tree of**
18 **life. We review the principles of phase separation and highlight how it impacts diverse**
19 **processes in the fungal kingdom. These include the regulation of autophagy, cell signaling**
20 **pathways, transcriptional circuits and the establishment of asymmetry in fungal cells. We**
21 **describe examples of stable, phase-separated assemblies including membrane-less organelles**
22 **(MLOs) such as the nucleolus, as well as transient condensates that also arise through phase**
23 **separation and enable cells to rapidly and reversibly respond to important environmental cues.**
24 **We showcase how research into phase separation in model yeasts, such as *Saccharomyces***
25 ***cerevisiae* and *Schizosaccharomyces pombe*, in conjunction with that in plant and human fungal**
26 **pathogens, such as *Ashbya gossypii* and *Candida albicans*, is continuing to enrich our**
27 **understanding of fundamental molecular processes.**

28

29 **INTRODUCTION**

30 Organelles are often bound by a lipid membrane that separates internal components from the
31 surrounding environment, but over the past decade multiple compartments have been identified in
32 which macromolecules are concentrated in the absence of a phospholipid membrane. Such membrane-
33 less organelles (MLOs) form by phase separation which involves de-mixing of a super-saturated
34 solution into a dense phase that exists together with a more dilute surrounding phase¹. Many MLOs
35 have liquid-like behaviour consistent with liquid-liquid phase separation (LLPS), and their components
36 can undergo rapid exchange with the surrounding environment^{2,3}. The physics of polymer systems
37 undergoing phase separation have been well studied through thermodynamic models such as the Flory-
38 Huggins theory⁴. When a polymer is mixed with a solvent, phase separation can occur above a crucial
39 concentration that depends on environmental factors (temperature, osmolarity, and pH) that alter the
40 effective favourability (free energy) of polymer-polymer interactions. MLOs that form via phase
41 separation take several forms, including liquid-like assemblies (via LLPS), semi-solid gels (with
42 viscoelastic behavior) and rigid fibrillar aggregates, and are associated with diverse cellular processes
43 throughout the fungal kingdom. A primer on the molecular forces underlying phase separation is
44 provided in BOX 1.

45 Here, we review the diverse roles of biomolecular condensates in model and pathogenic fungi,
46 including their function in autophagy, cytoskeletal organization and cell polarity, transcriptional
47 regulation of cell fate, and sensing and responding to the cellular environment.

48

49 ***Stress-induced bodies formed by phase separation***

50 Stress granules (SGs) and processing (P) bodies are dynamic MLOs that assemble on mRNAs
51 stalled in translation (FIG. 1). Different SGs can form depending on the stress, which leads to the
52 release of mRNAs encoding heat shock and chaperone factors thereby enabling their translation and
53 stress adaptation⁵. P bodies are constitutively present in the cytoplasm and share components with

54 SGs, but do not include translation initiation factors and instead sequester proteins associated with
55 mRNA decay⁶. SGs and P bodies therefore perform distinct functions, and these MLOs can also be
56 found docked against one another with mRNAs moving between them⁷. In *S. cerevisiae*, increased
57 temperature or depletion of specific nutrients triggers SG formation and is driven by high
58 concentrations of IDRs forming on mRNPs following stalled translation⁸. This causes the assembly of
59 condensates that then mature into a less dynamic, stable core that is surrounded by a liquid shell⁸.
60 Both yeast and mammalian SGs share a similar architecture, although a more extensive solid core in
61 yeast SGs makes them less dynamic overall^{8,9}.

62 *S. cerevisiae* poly(A)-binding protein Pab1 is a canonical SG factor that contains four RNA
63 recognition motifs (RRMs) as well as a proline-rich disordered domain (P domain)^{5,10}. Pab1 phase
64 separates *in vitro* to form gels in response to physiological cues such as a reduction in pH or heat
65 shock⁵. RRMs promote Pab1 phase separation through electrostatic interactions, while hydrophobic
66 interactions between P domains enhance this process⁵. A second *S. cerevisiae* SG protein, Pub1
67 (poly(U)-binding protein), is similar to Pab1 in that RRMs drive self-assembly while IDRs modify
68 condensate properties¹¹. Notably, Pub1 condensates show distinct material states depending on the
69 stress; purified Pub1 forms reversible, gel-like condensates in response to low pH whereas more solid-
70 like structures arise following heat shock, replicating observations with Pub1-containing condensates
71 in cells¹¹. Interestingly, only the more solid, thermally-induced condensates require the Hsp104
72 chaperone for dissolution¹¹ (FIG. 1), indicating differences in the structural architecture of these
73 condensates. Heat-induced condensates formed by Pab1 are similarly dispersed by an active
74 disaggregation system consisting of Hsp40/Hsp70/Hsp104 chaperones which therefore helps cells
75 recover from heat shock¹².

76 P bodies function in RNA metabolism including mRNA storage/decay, and are also induced by
77 stress¹³. These bodies are archetypal condensates with liquid-like properties both in *S. cerevisiae* and
78 in mammals, and several purified P body factors have been shown to undergo LLPS *in vitro*^{9,14,15}.

79 Multivalency in P bodies is achieved by interactions between folded protein domains, IDRs, and
80 RNA¹⁴. The most highly enriched P body proteins in *S. cerevisiae* (Dcp2, Pat1, and Edc3) partition
81 cooperatively into these bodies as well as promote P body assembly¹⁶ (FIG. 1). Importantly, these
82 studies suggest that only a few factors need to evolve LLPS capacity in order for MLOs to form¹⁶. In
83 heavily stressed cells, the liquidity of P bodies is maintained by Hsp104 and loss of this activity results
84 in P body proteins entering into SGs, further highlighting how disaggregases determine the behavior of
85 stress-induced MLOs in the cell⁹.

86 A third class of stress-induced condensate in *S. cerevisiae* is the glycolytic (G) body, which
87 involves glycolytic enzymes assembling into gel-like condensates during hypoxia^{17,18}. G bodies enable
88 growth under hypoxic conditions when oxidative phosphorylation is unavailable, most likely by
89 concentrating glycolytic enzymes within condensates and promoting glucose consumption¹⁸. G body
90 formation involves multivalent protein-protein and protein-RNA interactions and, as with other MLOs,
91 RNA may act as a scaffold for development of these bodies¹⁷. Additional factors recruited to G
92 bodies include Hsp70 chaperones (Ssa1/Ssa2) and the AMP-activated protein kinase Snf1p, with the
93 latter necessary for G body formation¹⁸. Analogous G-like bodies are present in human
94 hepatocarcinoma cells under hypoxic stress and where RNA enables the formation of these metabolic
95 bodies¹⁸, suggesting conservation across eukaryotes.

96

97 ***Changes to the cellular environment that drive phase separation***

98 Upon depletion of energy, *S. cerevisiae* and *S. pombe* yeast cells enter into a state of dormancy
99 associated with cytoplasmic acidification^{19,20}. The drop in intracellular pH occurs because culture
100 medium is acidic whereas the intracellular pH is neutral, and cells must expend energy to maintain this
101 pH difference^{21,22}. Energy depletion and intracellular acidification cause a number of cytoplasmic
102 proteins to assemble into microscopically visible foci or filaments^{19,23}. Under these conditions, the
103 yeast cytoplasm also transitions from its normal fluid state to a more solid-like state, which may be

104 because much of the yeast proteome becomes less soluble and forms higher order assemblies^{19,20,24}.
105 This response is not unique to yeast cells as bacterial cells similarly respond to glucose starvation by
106 transitioning from a glassy-liquid to a solid-like state, suggesting that these transitions are conserved
107 and promote adaptation to stress^{20,25}.

108 The *S. cerevisiae* translation termination factor Sup35, long studied for its ability to form a
109 heritable prion, also forms condensates upon a drop in intracellular pH²⁶. Sup35 consists of an N-
110 terminal prion-like domain (PrLD; see BOX 1), a negatively charged middle (M) domain, and a C-
111 terminal GTPase domain that catalyzes translation termination. Franzmann *et al.* showed that the M-
112 domain acts as a pH sensor and causes Sup35 to form gel-like droplets following a stress-induced pH
113 reduction, and that droplets redissolve upon restoration of pH, both *in vitro* and in cells²⁶. In contrast,
114 the Sup35 C-terminal domain forms irreversible aggregates during stress when expressed alone, as the
115 PrLD is necessary for preventing aggregate formation. Reversible gel formation appears to be the
116 ancestral role of Sup35, as the *S. pombe* ortholog cannot propagate as a prion but shares the ability to
117 form stress-induced condensates²⁶. Thus, most PrLDs (*S. cerevisiae* contains >200 proteins with such
118 domains) likely function to modulate phase separation or protein solubility rather than act as prions,
119 with the latter being the exception rather than the rule²⁷. Debate continues as to the relative importance
120 of *S. cerevisiae* Sup35 in forming condensates versus the prion state, with both roles being potentially
121 beneficial to this species²⁸.

122 Related studies have demonstrated that increased macromolecular crowding can promote phase
123 separation events. Crowding agents such as polyethylene glycol have been extensively used to
124 increase effective protein concentrations and promote phase separation *in vitro*²⁹. To examine how
125 macromolecular crowding influences behavior within cells, Delarue *et al.* performed microscopic
126 tracking of genetically encoded multimeric (GEM) nanoparticles³⁰. GEMs consist of a fluorescent
127 molecule fused to a scaffold which multimerizes into particles of a defined shape and size. When
128 expressed in *S. cerevisiae* cells, the motility of GEMs was reduced in the relatively crowded nucleus

129 compared to that in the cytoplasm³¹ (FIG. 2a). Using this system, increased mTORC1 activity was
130 shown to increase macromolecular crowding due to an increase in ribosome number³⁰ (FIG. 2b).
131 Ribosomes are a major cellular component (~200,000 ribosomes are present per yeast cell) and occupy
132 ~20% of the cytosolic volume; an increase in the number of ribosomes therefore increased both
133 macromolecular crowding and phase separation of a cytosolic protein³⁰. These experiments establish
134 close links between ribosome concentrations, macromolecular crowding and phase separation in yeast,
135 with similar results obtained in a human cell line³⁰. A recent study showed that increased
136 macromolecular crowding also occurs in energy-starved *S. cerevisiae* cells due to a reduction in cell
137 size, which in turn supports the formation of MLOs²⁴.

138 Taken together, these studies reveal that starvation can drive phase separation and
139 oligomerization of cellular factors due to both changes in intracellular pH and increased molecular
140 crowding. Recent experiments further show that hyperosmotic stress can also drive the formation of
141 intracellular protein foci (OSF; osmotic shock foci) which may represent liquid droplets formed upon
142 increased intracellular crowding³². Given that biocondensates arise in response to multiple stresses, it
143 is important to note that protein constituents can be shared between different stress-induced
144 condensates. For example, Sup35 and the SG protein Pab1 partially colocalize in pH-stressed cells but
145 not in starvation-stressed cells²⁶. A key ongoing research question is to therefore determine what
146 controls the targeting of molecules to different stress-induced condensates in the cell.

147

148 ***The cytoskeleton, cell polarity and control of nuclear division***

149 The cytoskeleton is a dynamic structure composed of filaments that undergo nucleation,
150 polymerization, and depolymerization. In both budding yeast and filamentous fungi, the polarisome
151 nucleates actin polymerization which involves the formin protein Bni1 together with nucleation
152 promoting factor (NPF) and the scaffold protein Spa2^{33,34}. In *S. cerevisiae*, polarisome proteins
153 concentrate at the bud tip via LLPS to nucleate actin assembly while remaining in exchange with the

154 surrounding cytoplasm^{34,35}. Xie *et al.* identified actin-interacting protein 5 (Aip5) as a factor that
155 synergistically promotes actin assembly with Bni1³⁴. Intriguingly, the N-terminal domain of Aip5 is
156 an IDR that causes the formation of amorphous condensates *in vitro*, while addition of Spa2 to Aip5
157 assemblies turns these condensates into more dynamic, liquid-like droplets^{34,35}. It is therefore
158 envisaged that Spa2 prevents Aip5 aggregation during stress, which in turn enables condensate
159 dissolution and supports the restart of actin assembly during recovery from stress^{34,35} (FIG. 3a).

160 *Ashbya gossypii* is a filamentous fungus that is a plant pathogen and, like *S. cerevisiae*, belongs
161 to the family *Saccharomycetaceae*. *A. gossypii* has emerged as an important model organism for
162 studying cell polarity, filamentation and how asynchronous nuclear divisions occur within
163 multinucleated cells. Remarkably, the protein Whi3 has been linked to the regulation of both cell
164 polarity and the timing of nuclear divisions due to its ability to form RNA-dependent liquid droplets³⁶
165³⁸ (FIG. 3b). Whi3 establishes polarity at symmetry breaking points in the cell by forming condensates
166 with Puf2 that incorporate *BN11* and *SPA2* RNA transcripts^{36,37}. In contrast, Whi3 droplets near nuclei
167 contain *CLN3* mRNA (encoding for a G1 regulatory cyclin), and differences in the spatial distribution
168 of this transcript determine the timing of the nuclear divisions in multinucleate cells^{36,38}. Zhang *et al.*
169 showed that the presence of different mRNAs results in distinct types of Whi3 condensates, from more
170 liquid-like to more gel-like assemblies³⁶. These results therefore provide a striking example of how
171 RNA can impact the physical properties of biocondensates and can result in changes in their size,
172 shape, viscosity, surface tension and composition^{36,39} (also see BOX 2 for the central role of nucleic
173 acids in promoting phase separation).

174

175 *Autophagy*

176 Autophagy is the organized breakdown of components by the lysosome, and provides energy
177 and building blocks for cells to survive stress. This process involves formation of the Pre-
178 Autophagosomal Structure (PAS) on the cytoplasmic face of the vacuolar membrane, which nucleates

179 assembly of a cup-shaped isolation membrane adjacent to the PAS that engulfs material in an
180 autophagosome^{40,41}. *S. cerevisiae* PAS formation involves five IDR-containing Atg (autophagy-
181 related) proteins that co-assemble into the ATG1 complex (FIG. 4a)⁴⁰⁻⁴². In starved cells, the TORC1
182 kinase is inactivated and Atg13 becomes dephosphorylated (by PP2C phosphatases) and establishes
183 multivalent interactions with Atg17 to form highly liquid droplets^{42,43}. Atg13 also interacts with the
184 Vac8 membrane protein to anchor ATG1 droplets at the vacuolar membrane where they fuse to form
185 one large condensate – the PAS^{40,42}. Within the PAS, Atg1 is activated by autophosphorylation and
186 phosphorylates Atg13, creating an equilibrium between phospho-Atg13 in the dilute phase and its
187 unphosphorylated form in the condensed phase, which is important for maintenance of the PAS⁴² (FIG.
188 4a). Formation of the cupped isolation membrane is not fully understood but is initiated by the
189 recruitment of Atg9-containing vacuoles to the PAS via interactions with Atg13, and these vacuoles
190 then fuse to generate the isolation membrane^{44,45} (FIG. 4a). ATG proteins are conserved and phase
191 separation is likely to play related roles in autophagy in multicellular organisms and yeast, although
192 autophagosome formation is organized differently (both spatially and temporally) between these
193 species⁴¹.

194 A distinct form of autophagy, selective autophagy, targets specific organelles and biomolecules
195 to the vacuole even under nutrient-rich conditions and also involves phase separation. *S. cerevisiae*
196 Ape1 is the principle cargo of a form of selective autophagy termed the cytoplasm-to-vacuole targeting
197 (Cvt) pathway^{41,46}. Ape1 contains an N-terminal propeptide that can form a helical structure and self-
198 assemble into dodecamers that then coalesce into semi-liquid droplets⁴⁶⁻⁴⁸. Atg19 acts as a receptor for
199 Ape1 as it “floats” on the surface of Ape1 condensates and connects these condensates to Atg8/Atg21
200 (Fig. 4b)⁴⁶⁻⁴⁸. Through these interactions, a shape change in the isolation membrane enables it to form
201 a phospholipid bilayer around Ape1 droplets and sequester them for degradation⁴⁷. Changing a single
202 amino acid in the Ape1 propeptide produced amorphous aggregates rather than gel-like droplets, and
203 these hardened structures failed to interact with Atg19/Atg8 or undergo autophagy⁴⁷. Similar results

204 have been observed in the targeting of *Caenorhabditis elegans* P granule proteins for autophagic
205 degradation, where the gel-like state provides a suitable platform for engulfment by autophagosomal
206 membranes⁴⁹. These results highlight how the material properties of condensates are critical for
207 determining the destination of cellular cargoes, both in fungi and higher eukaryotes.

208

209 ***Regulation of autophagy via sensing of reactive oxygen species***

210 *S. cerevisiae* cells switched from a nutrient-rich medium to a minimal medium containing a
211 non-fermentable carbon source undergo autophagy even in the continued presence of nitrogen, which
212 can help cells maintain mitochondrial health during respiratory growth⁵⁰. Tu and colleagues revealed
213 that reactive oxygen species (ROS) produced by high mitochondrial dysfunction under these
214 conditions are sensed by Pbp1, the yeast ortholog of mammalian ataxin-2^{51,52}. Remarkably, Pbp1 is
215 capable of undergoing phase separation in a redox-sensitive manner; this protein readily forms liquid-
216 or gel-like droplets *in vitro* but these droplets dissolve upon the addition of hydrogen peroxide⁵¹. This
217 mechanism involves oxidation of methionine residues within the Pbp1 LCR which therefore acts as a
218 reversible readout of mitochondrial respiratory status⁵¹. Thus, Pbp1 condensates form during high
219 respiratory growth and are poised to sense mitochondrial dysfunction and increased ROS levels, which
220 in turn results in activation of TORC1 and inhibition of autophagy (as a means of adaptation to
221 mitochondrial stress)^{52,53}. These studies provide a striking example of how phase separation can be
222 tuned by key physiological signals such as ROS. It was subsequently shown that human TDP-43
223 (involved in the formation of neuronal granules) similarly forms redox-sensitive condensates⁵⁴,
224 highlighting how observations in *S. cerevisiae* led to the discovery of ROS sensing via phase
225 separation in higher organisms.

226

227 ***Phase separation as a mechanism for sensing carbon dioxide***

228 Cells have evolved sensitive mechanisms to detect changes in the levels of carbon dioxide

229 (CO₂). In fungi, CO₂ can affect multiple processes including mating, meiosis, phenotypic switching
230 and filamentation⁵⁵. Zhang *et al.* revealed that CO₂ sensing in the opportunistic human fungal
231 pathogen *Candida albicans* involves condensates formed by Ptc2, a member of the PP2C family of
232 phosphatases⁵⁶. Here, a serine/threonine-rich region within the IDR of Ptc2 enabled this protein to
233 undergo CO₂-induced phase separation, with CO₂ envisaged as a “molecular glue” that bridges
234 interactions between Ptc2 molecules thereby stimulating condensate formation⁵⁶. A related PP2C
235 phosphatase from plants showed a similar ability to undergo CO₂-induced phase separation⁵⁶,
236 indicating that this mechanism of environmental sensing (while uncovered in fungi) is likely conserved
237 across diverse eukaryotic species⁵⁶.

238

239 ***Nuclear compartmentalization and heterochromatin***

240 Phase separation plays a central role in the establishment of nuclear compartments such as the
241 nucleolus which houses ribosome biogenesis and ribonucleoprotein assembly. This organelle is
242 organized into three nested sub-compartments in higher eukaryotes; a core fibrillar center (FC) exists
243 inside a dense fibrillar component (DFC), which itself resides within the granular component (GC)⁵⁷.
244 These compartments represent coexisting, immiscible liquid phases – this layered, multiphase
245 architecture was reproduced *in vitro* as coincubation of a DFC protein with a GC protein generated
246 multiphase droplets⁵⁷. Here, IDRs within these proteins drive phase separation while RNA binding
247 domains contribute to the immiscibility of the protein phases⁵⁷. *S. cerevisiae* nucleoli have only two
248 sub-compartments⁵⁸ and modeling suggests that ribosomal DNA (rDNA) is phase separated from bulk
249 chromatin due to crosslinks between rDNA repeats⁵⁹, while nucleolar RNPs also undergo phase
250 separation⁶⁰. Indeed, the combination of rDNA phase separation and tethering of rDNA repeats to the
251 nuclear envelope may explain the characteristic crescent shape of the yeast nucleolus⁶¹.

252 Phase separation also controls the formation of transcriptionally repressed heterochromatin.

253 Pioneering work on heterochromatin protein 1 (HP1) in higher eukaryotes showed that it can undergo

254 phase separation and recruit other heterochromatin-associated factors involved in transcriptional
255 repression^{62,63}. Constitutive heterochromatin is marked by trimethylation of lysine 9 on histone H3
256 (H3K9me3), and interactions between these marks and both HP1 chromodomains and SUV39H1
257 (which introduces H3K9me3 marks) are drivers of phase separation⁶⁴. DNA polymers also contribute
258 to the properties of heterochromatin resulting in stable structures that resist mechanical forces, while
259 HP1 can exchange between condensate and non-condensate populations⁶⁵. Swi6, the *S. pombe*
260 homolog of HP1, similarly undergoes phase separation with reconstituted chromatin that contains
261 H3K9me3 marks, suggesting parallels between constitutive heterochromatin formation in yeast and
262 humans⁶⁴. Related mechanisms may establish the formation of facultative heterochromatin in which
263 polycomb proteins form phase-separated condensates and are associated with chromatin that is
264 trimethylated on lysine 27 of histone H3 (H3K27me3)^{66,67}.

265

266 ***Phase separation, transcriptional activation and super-enhancer-like elements***

267 Multiple studies have observed that transcription factors (TFs) can assemble into phase-
268 separated complexes to activate gene expression⁶⁸⁻⁷². Phase separation may occur preferentially at
269 mammalian super-enhancers (SEs), where high concentrations of TFs, Mediator complex and RNA
270 polymerase II (Pol II) span genomic regions >10 kb^{69,70,72} (FIG. 5a,b). Weak multivalent interactions
271 between TFs and coactivators together with structured interactions between TFs and DNA promote
272 phase separation⁷⁰. The sharply defined thresholds associated with condensate formation may underlie
273 unique SE properties such as their hypersensitivity to changes in TF levels⁶⁹. Moreover, the *de novo*
274 assembly of a SE can be initiated by binding of a single TF to an enhancer, as exemplified by somatic
275 mutations that cause MYB binding and subsequent TAL1 overexpression in T-cell acute lymphoblastic
276 leukemia⁷³.

277 Mammalian SEs have been linked to transcriptional regulatory networks (TRNs) that define
278 cell fate, where a core set of master TFs act in concert to control the expression of large numbers of

279 target genes^{74,75}. Intriguingly, fungal TRNs are also regulated by sets of master TFs operating at super-
280 sized regulatory regions (“SE-like elements”). Prominent examples of fungal TRNs include those
281 regulating pseudohyphal formation in *S. cerevisiae*, the temperature response in *Histoplasma*
282 *capsulatum*, biofilm formation and phenotypic switching in *C. albicans*, and the heat shock response
283 that is conserved from fungi to humans⁷⁶⁻⁷⁹. The TRN regulating white-opaque phenotypic switching
284 in *C. albicans* has been extensively analyzed and involves eight master TFs that act together at SE-like
285 elements^{80,81} (FIG. 5c,d). The master white-opaque TFs are often recruited to SE-like regions even in
286 the absence of consensus DNA binding motifs, indicating they are likely recruited via protein-protein
287 interactions. These regulatory TFs contain PrLDs that enable them to undergo phase separation *in*
288 *vitro*, and mutations that block this process abolish their function, thereby linking phase separation to
289 the regulation of this TRN⁸². Analysis of the heat shock response in *S. cerevisiae* similarly shows the
290 presence of SE-like elements at which transcriptional condensates are expected to form^{83,84}. Phase
291 separation and SE-like regions are therefore implicated in transcriptional regulation in both fungi and
292 mammals, as compared in TABLE 1.

293 Despite considerable interest in SEs it is currently unclear whether these elements are
294 functionally distinct from regular enhancers, and the role of phase separation in transcription is also
295 strongly debated^{85,86}. Indeed, a recent study suggests that multivalent interactions can enable the
296 formation of mammalian TF “hubs” that promote gene expression, yet when hubs assemble into larger,
297 phase-separated condensates then gene expression is inhibited⁸⁷. These results support a “Goldilocks”
298 model whereby small changes in multivalent interactions can finely tune gene activation up or down,
299 but where formation of condensates results in transcription inhibition⁸⁷. Clearly, more work is required
300 in this exciting area and examination of gene context will be critical, with condensates potentially
301 enabling transcription at certain loci while restricting it at others. Additional technological innovations
302 are therefore needed to further dissect the role of phase separation in transcription, including improved
303 techniques to evaluate proteins by high resolution microscopy when expressed at endogenous levels in

304 live cells.

305

306 ***Regulation of RNA polymerase II via phase separation***

307 RNA Pol II contains a conserved, intrinsically disordered C-terminal domain (CTD) that
308 enables it to form condensates, as well as to co-phase separate with transcription factors and
309 transcriptional machinery⁸⁸⁻⁹¹. The longer length of the mammalian CTD relative to the *S. cerevisiae*
310 CTD (52 v. 26 heptad repeats) results in an increased propensity to undergo phase separation due to
311 stronger CTD-CTD interactions⁸⁸. CTD phosphorylation leads to dissociation of Pol II from Mediator
312 condensates (associated with transcription initiation) and recruitment into condensates containing
313 splicing factors⁹¹ (FIG. 5e). These transitions could involve direct maturation of Pol II-containing
314 condensates or Pol II exiting initiation condensates before recruitment to splicing condensates⁹².

315 Related to this work, Quintero-Cadena *et al.* showed that Pol II CTD length correlates with
316 gene density in eukaryotes, and proposed that this domain serves as a molecular bridge for Pol II to be
317 recruited to active promoters, with longer CTD lengths enabling recruitment across greater distances⁹³.
318 CTD length also modulated transcriptional bursting with longer CTDs leading to stronger and more
319 frequent bursts. Surprisingly, a truncated *S. cerevisiae* CTD was non-functional but function was
320 restored by fusion to phase-separating IDRs from human FUS or TAF15 proteins⁹³. Together, these
321 studies demonstrate that CTD-CTD interactions, as well as CTD interactions with TFs, coactivators,
322 and Mediator, assist the recruitment of Pol II for gene transcription.

323 RNA plays an integral role in transcriptional phase separation; low RNA levels increase the
324 formation of Mediator condensates whereas high RNA levels dissolve these condensates⁹⁴. This may
325 result in a feedback mechanism whereby transcription dissipates condensates and causes the
326 transcriptional bursts that are characteristic of this process⁹⁴. Moreover, promoter-associated RNAs in
327 mammalian cells are likely bound by multiple RBPs that enable Pol II and cofactors to reach the
328 threshold levels necessary for phase separation⁹⁵, and certain RBPs also promote Pol II release from

329 initiation complexes to support transcription elongation⁹⁶.

330 Recent studies in *S. cerevisiae* have similarly shown that TBP associated factor 14 (Taf14; a
331 component of TFIID and chromatin remodeling complexes) utilizes multiple interaction partners to
332 regulate transcription. Chen *et al.* demonstrated that a structured extra-terminal (ET) domain of Taf14
333 recruits co-factors via an ET-binding motif present on these partners⁹⁷. Moreover, Taf14 formed
334 condensates *in vitro* and binding partners could partition into these droplets, establishing that Taf14
335 can act as a scaffold to bring together co-factors and drive gene expression⁹⁷. While the formation of
336 phase-separated hubs is a recurring theme in transcription, Taf14 is, so far, an unusual example of a
337 transcriptional regulator that is reported to use only structured domains to scaffold multi-component,
338 phase-separated condensates⁹⁷.

339

340 ***Fungi as model species to study amyloid disease***

341 In addition to endogenous phase separation phenomena, fungi have been used to model the
342 properties (and toxicities) of aggregative amyloids implicated in human disease^{98,99}. In many cases,
343 the precise role of condensate or amyloid formation in neurodegenerative diseases such as
344 Huntington's, amyotrophic lateral sclerosis (ALS), Alzheimer's and Parkinson's is uncertain, although
345 disease-causing mutations often increase amyloid formation in proteins associated with each
346 disease^{100,101}.

347 Several aggregation-prone human proteins have been analyzed in *S. cerevisiae*, with high-
348 throughput screening used to identify new therapeutics that reduce amyloid toxicity^{102,103}. Yeast have
349 also been invaluable in studying disaggregases that can detoxify aggregation-prone proteins
350 associated with neurodegeneration. For example, *S. cerevisiae* Hsp104, or variants of this chaperone,
351 can not only act as disaggregases (or anti-aggregation activities) on endogenous proteins but are also
352 functional on human proteins associated with neurologic disorders despite metazoans lacking an
353 ortholog of Hsp104^{104,105}. Model fungi and yeast genetics therefore continue to be used to understand

354 how aberrant phase transitions/aggregation can impact neurodegenerative diseases and to develop
355 therapeutic interventions.

356

357 **Conclusions**

358 Phase separation and the formation of biomolecular condensates play central roles in virtually
359 all aspects of biology, from ubiquitous cellular compartments to highly inducible assemblies. In fungi,
360 the formation of condensates is highly sensitive to cellular conditions and phase separation therefore
361 acts as an exquisite sensor of environmental cues, as evidenced in the responses to changes in pH, ROS
362 and CO₂ levels. Outstanding questions with regards to phase separation and MLOs in fungi include a
363 better understanding of the molecular interactions that nucleate and stabilize phase separation; the
364 contribution of transient or stable secondary structures to condensate formation; understanding the
365 specificity by which proteins/nucleic acids are recruited to condensates; new tools to examine phase
366 separation of proteins at endogenous levels in fungal cells; determination of which small molecules
367 impact condensates; and developing therapeutic approaches including antifungal drugs based on
368 understanding of phase separation biology. Studies in fungi will continue to be at the forefront of this
369 field given the cell biological and genetic tools available in model fungi and the diversity of species
370 being studied both as model organisms and as plant and human pathogens.

371

372

373 **Acknowledgements**

374 We would like to thank members of the Bennett lab for useful discussions and Dr. Benjamin Tu
375 (UTSW) for feedback on sections of the review. Work in the Bennett lab is supported by NIAID
376 grants AI141893/AI081704/AI166869 and work in the Fawzi lab is supported by NSF BIO 1845734
377 and NINDS R01NS116176.

378

379 **Contributions**

380 MIS wrote the initial draft which was extensively revised by RJB and CF, with input from NLF.

381

382 **Competing interests**

383 NLF is a member of the scientific advisory board of Dewpoint Therapeutics.

384

385

386 **References**

387 1 Boeynaems, S. *et al.* Protein phase separation: A new phase in cell biology. *Trends Cell Biol*
388 **28**, 420-435, doi:10.1016/j.tcb.2018.02.004 (2018).

389 2 Gomes, E. & Shorter, J. The molecular language of membraneless organelles. *J Biol Chem* **294**,
390 7115-7127, doi:10.1074/jbc.TM118.001192 (2019).

391 3 Shin, Y. & Brangwynne, C. P. Liquid phase condensation in cell physiology and disease.
392 *Science* **357**, doi:10.1126/science.aaf4382 (2017).

393 4 Mitrea, D. M. & Kriwacki, R. W. Phase separation in biology; functional organization of a
394 higher order. *Cell communication and signaling : CCS* **14**, 1, doi:10.1186/s12964-015-0125-7
395 (2016).

396 5 Riback, J. A. *et al.* Stress-triggered phase separation is an adaptive, evolutionarily tuned
397 response. *Cell* **168**, 1028-1040 e1019, doi:10.1016/j.cell.2017.02.027 (2017).

398 6 Ivanov, P., Kedersha, N. & Anderson, P. Stress granules and processing bodies in translational
399 control. *Cold Spring Harbor perspectives in biology* **11**, doi:10.1101/cshperspect.a032813
400 (2019).

401 7 Moon, S. L. *et al.* Multicolour single-molecule tracking of mRNA interactions with RNP
402 granules. *Nature cell biology* **21**, 162-168, doi:10.1038/s41556-018-0263-4 (2019).

403 8 Jain, S. *et al.* ATPase-modulated stress granules contain a diverse proteome and substructure.
404 *Cell* **164**, 487-498, doi:10.1016/j.cell.2015.12.038 (2016).

405 9 Kroschwitz, S. *et al.* Promiscuous interactions and protein disaggregases determine the
406 material state of stress-inducible RNP granules. *eLife* **4**, e06807, doi:10.7554/eLife.06807
407 (2015).

408 10 Anderson, P. & Kedersha, N. RNA granules. *J Cell Biol* **172**, 803-808,
409 doi:10.1083/jcb.200512082 (2006).

410 11 Kroschwitzl, S. *et al.* Different material states of Pub1 condensates define distinct modes of
411 stress adaptation and recovery. *Cell Reports* **23**, 3327-3339, doi:10.1016/j.celrep.2018.05.041
412 (2018).

413 12 Yoo, H., Bard, J. A. M., Pilipenko, E. V. & Drummond, D. A. Chaperones directly and
414 efficiently disperse stress-triggered biomolecular condensates. *Mol Cell* **82**, 741-755 e711,
415 doi:10.1016/j.molcel.2022.01.005 (2022).

416 13 Luo, Y., Na, Z. & Slavoff, S. A. P-Bodies: Composition, properties, and functions.
417 *Biochemistry* **57**, 2424-2431, doi:10.1021/acs.biochem.7b01162 (2018).

418 14 Schutz, S., Noldeke, E. R. & Sprangers, R. A synergistic network of interactions promotes the
419 formation of *in vitro* processing bodies and protects mRNA against decapping. *Nucleic Acids*
420 *Res*, doi:10.1093/nar/gkx353 (2017).

421 15 Fromm, S. A. *et al.* In vitro reconstitution of a cellular phase-transition process that involves
422 the mRNA decapping machinery. *Angew Chem Int Ed Engl* **53**, 7354-7359,
423 doi:10.1002/anie.201402885 (2014).

424 16 Xing, W., Muhlrad, D., Parker, R. & Rosen, M. K. A quantitative inventory of yeast P body
425 proteins reveals principles of composition and specificity. *eLife* **9**, doi:10.7554/eLife.56525
426 (2020).

427 17 Fuller, G. G. *et al.* RNA promotes phase separation of glycolysis enzymes into yeast G bodies
428 in hypoxia. *eLife* **9**, doi:10.7554/eLife.48480 (2020).

429 18 Jin, M. *et al.* Glycolytic enzymes coalesce in G bodies under hypoxic stress. *Cell reports* **20**,
430 895-908, doi:10.1016/j.celrep.2017.06.082 (2017).

431 19 Munder, M. C. *et al.* A pH-driven transition of the cytoplasm from a fluid- to a solid-like state
432 promotes entry into dormancy. *eLife* **5**, doi:10.7554/eLife.09347 (2016).

433 20 Joyner, R. P. *et al.* A glucose-starvation response regulates the diffusion of macromolecules.
434 *eLife* **5**, doi:10.7554/eLife.09376 (2016).

435 21 Dechant, R. *et al.* Cytosolic pH is a second messenger for glucose and regulates the PKA
436 pathway through V-ATPase. *EMBO J* **29**, 2515-2526, doi:10.1038/emboj.2010.138 (2010).

437 22 Orij, R., Postmus, J., Ter Beek, A., Brul, S. & Smits, G. J. *In vivo* measurement of cytosolic
438 and mitochondrial pH using a pH-sensitive GFP derivative in *Saccharomyces cerevisiae*
439 reveals a relation between intracellular pH and growth. *Microbiology (Reading)* **155**, 268-278,
440 doi:10.1099/mic.0.022038-0 (2009).

441 23 Petrovska, I. *et al.* Filament formation by metabolic enzymes is a specific adaptation to an
442 advanced state of cellular starvation. *eLife*, doi:10.7554/eLife.02409 (2014).

443 24 Marini, G., Nuske, E., Leng, W., Alberti, S. & Pigino, G. Reorganization of budding yeast
444 cytoplasm upon energy depletion. *Mol Biol Cell* **31**, 1232-1245, doi:10.1091/mbc.E20-02-0125
445 (2020).

446 25 Parry, B. R. *et al.* The bacterial cytoplasm has glass-like properties and is fluidized by
447 metabolic activity. *Cell* **156**, 183-194, doi:10.1016/j.cell.2013.11.028 (2014).

448 26 Franzmann, T. M. *et al.* Phase separation of a yeast prion protein promotes cellular fitness.
449 *Science* **359**, doi:10.1126/science.aoa5654 (2018).

450 27 Franzmann, T. M. & Alberti, S. Prion-like low-complexity sequences: Key regulators of
451 protein solubility and phase behavior. *J Biol Chem* **294**, 7128-7136,
452 doi:10.1074/jbc.TM118.001190 (2019).

453 28 Lyke, D. R., Dorweiler, J. E. & Manogaran, A. L. The three faces of Sup35. *Yeast* **36**, 465-472,
454 doi:10.1002/yea.3392 (2019).

455 29 Andre, A. A. M. & Spruijt, E. Liquid-liquid phase separation in crowded environments.
456 *International Journal of Molecular Sciences* **21**, doi:10.3390/ijms21165908 (2020).

457 30 Delarue, M. *et al.* mTORC1 controls phase separation and the biophysical properties of the
458 cytoplasm by tuning crowding. *Cell* **174**, 338-349 e320, doi:10.1016/j.cell.2018.05.042 (2018).

459 31 Shu, T. *et al.* nucGEMs probe the biophysical properties of the nucleoplasm. *bioRxiv*,
460 2021.2011.2018.469159, doi:10.1101/2021.11.18.469159 (2022).

461 32 Alexandrov, A. I. *et al.* Analysis of novel hyperosmotic shock response suggests 'beads in
462 liquid' cytosol structure. *Biol Open* **8**, doi:10.1242/bio.044529 (2019).

463 33 Liu, B. *et al.* The polarisome is required for segregation and retrograde transport of protein
464 aggregates. *Cell* **140**, 257-267, doi:10.1016/j.cell.2009.12.031 (2010).

465 34 Xie, Y. *et al.* Polarisome scaffold Spa2-mediated macromolecular condensation of Aip5 for
466 actin polymerization. *Nature Communications* **10**, 5078, doi:10.1038/s41467-019-13125-1
467 (2019).

468 35 Xie, Y. & Miao, Y. Polarisome assembly mediates actin remodeling during polarized yeast and
469 fungal growth. *J Cell Sci* **134**, doi:10.1242/jcs.247916 (2021).

470 36 Zhang, H. *et al.* RNA controls polyQ protein phase transitions. *Mol Cell* **60**, 220-230,
471 doi:10.1016/j.molcel.2015.09.017 (2015).

472 37 Lee, C., Occhipinti, P. & Gladfelter, A. S. PolyQ-dependent RNA-protein assemblies control
473 symmetry breaking. *J Cell Biol* **208**, 533-544, doi:10.1083/jcb.201407105 (2015).

474 38 Lee, C. *et al.* Protein aggregation behavior regulates cyclin transcript localization and cell-cycle
475 control. *Dev Cell* **25**, 572-584, doi:10.1016/j.devcel.2013.05.007 (2013).

476 39 Roden, C. & Gladfelter, A. S. RNA contributions to the form and function of biomolecular
477 condensates. *Nature Reviews. Molecular Cell Biology* **22**, 183-195, doi:10.1038/s41580-020-
478 0264-6 (2021).

479 40 Nakatogawa, H., Suzuki, K., Kamada, Y. & Ohsumi, Y. Dynamics and diversity in autophagy
480 mechanisms: lessons from yeast. *Nature Reviews. Molecular Cell Biology* **10**, 458-467,
481 doi:10.1038/nrm2708 (2009).

482 41 Noda, N. N., Wang, Z. & Zhang, H. Liquid-liquid phase separation in autophagy. *J Cell Biol*
483 **219**, doi:10.1083/jcb.202004062 (2020).

484 42 Fujioka, Y. *et al.* Phase separation organizes the site of autophagosome formation. *Nature* **578**,
485 301-305, doi:10.1038/s41586-020-1977-6 (2020).

486 43 Yamamoto, H. *et al.* The intrinsically disordered protein Atg13 mediates supramolecular
487 assembly of autophagy initiation complexes. *Dev Cell* **38**, 86-99,
488 doi:10.1016/j.devcel.2016.06.015 (2016).

489 44 Yamamoto, H. *et al.* Atg9 vesicles are an important membrane source during early steps of
490 autophagosome formation. *J Cell Biol* **198**, 219-233, doi:10.1083/jcb.201202061 (2012).

491 45 Suzuki, S. W. *et al.* Atg13 HORMA domain recruits Atg9 vesicles during autophagosome
492 formation. *Proc Natl Acad Sci U S A* **112**, 3350-3355, doi:10.1073/pnas.1421092112 (2015).

493 46 Yamasaki, A. & Noda, N. N. Structural biology of the Cvt pathway. *J Mol Biol* **429**, 531-542,
494 doi:10.1016/j.jmb.2017.01.003 (2017).

495 47 Yamasaki, A. *et al.* Liquidity is a critical determinant for selective autophagy of protein
496 condensates. *Mol Cell* **77**, 1163-1175 e1169, doi:10.1016/j.molcel.2019.12.026 (2020).

497 48 Yamasaki, A. *et al.* Structural basis for receptor-mediated selective autophagy of
498 aminopeptidase I aggregates. *Cell Reports* **16**, 19-27, doi:10.1016/j.celrep.2016.05.066 (2016).

499 49 Zhang, G., Wang, Z., Du, Z. & Zhang, H. mTOR regulates phase separation of PGL granules to
500 modulate their autophagic degradation. *Cell* **174**, 1492-1506 e1422,
501 doi:10.1016/j.cell.2018.08.006 (2018).

502 50 Wu, X. & Tu, B. P. Selective regulation of autophagy by the Iml1-Npr2-Npr3 complex in the
503 absence of nitrogen starvation. *Mol Biol Cell* **22**, 4124-4133, doi:10.1091/mbc.E11-06-0525
504 (2011).

505 51 Kato, M. *et al.* Redox state controls phase separation of the yeast ataxin-2 protein via reversible
506 oxidation of its methionine-rich low-complexity domain. *Cell* **177**, 711-721 e718,
507 doi:10.1016/j.cell.2019.02.044 (2019).

508 52 Yang, Y. S. *et al.* Yeast ataxin-2 forms an intracellular condensate required for the inhibition of
509 TORC1 signaling during respiratory growth. *Cell* **177**, 697-710 e617,
510 doi:10.1016/j.cell.2019.02.043 (2019).

511 53 Prouteau, M. & Loewith, R. TOR signaling is going through a phase. *Cell Metab* **29**, 1019-
512 1021, doi:10.1016/j.cmet.2019.04.010 (2019).

513 54 Lin, Y. *et al.* Redox-mediated regulation of an evolutionarily conserved cross-beta structure
514 formed by the TDP43 low complexity domain. *Proc Natl Acad Sci U S A* **117**, 28727-28734,
515 doi:10.1073/pnas.2012216117 (2020).

516 55 Martin, R., Pohlers, S., Muhlschlegel, F. A. & Kurzai, O. CO₂ sensing in fungi: at the heart of
517 metabolic signaling. *Curr Genet* **63**, 965-972, doi:10.1007/s00294-017-0700-0 (2017).

518 56 Zhang, M. *et al.* The intrinsically disordered region from PP2C phosphatases functions as a
519 conserved CO₂ sensor. *Nature Cell Biology* **24**, 1029-1037, doi:10.1038/s41556-022-00936-6
520 (2022).

521 57 Feric, M. *et al.* Coexisting liquid phases underlie nucleolar subcompartments. *Cell* **165**, 1686-
522 1697, doi:10.1016/j.cell.2016.04.047 (2016).

523 58 Thiry, M. & Lafontaine, D. L. Birth of a nucleolus: the evolution of nucleolar compartments.
524 *Trends Cell Biol* **15**, 194-199, doi:10.1016/j.tcb.2005.02.007 (2005).

525 59 Hult, C. *et al.* Enrichment of dynamic chromosomal crosslinks drive phase separation of the
526 nucleolus. *Nucleic Acids Res* **45**, 11159-11173, doi:10.1093/nar/gkx741 (2017).

527 60 Lawrimore, J. *et al.* The rDNA is biomolecular condensate formed by polymer-polymer phase
528 separation and is sequestered in the nucleolus by transcription and R-loops. *Nucleic Acids Res*
529 **49**, 4586-4598, doi:10.1093/nar/gkab229 (2021).

530 61 Hall, A. C., Ostrowski, L. A. & Mekhail, K. Phase separation as a melting pot for DNA repeats.
531 *Trends Genet* **35**, 589-600, doi:10.1016/j.tig.2019.05.001 (2019).

532 62 Larson, A. G. *et al.* Liquid droplet formation by HP1alpha suggests a role for phase separation
533 in heterochromatin. *Nature* **547**, 236-240, doi:10.1038/nature22822 (2017).

534 63 Strom, A. R. *et al.* Phase separation drives heterochromatin domain formation. *Nature* **547**,
535 241-245, doi:10.1038/nature22989 (2017).

536 64 Wang, L. *et al.* Histone modifications regulate chromatin compartmentalization by contributing
537 to a phase separation mechanism. *Mol Cell* **76**, 646-659 e646,
538 doi:10.1016/j.molcel.2019.08.019 (2019).

539 65 Keenen, M. M. *et al.* HP1 proteins compact DNA into mechanically and positionally stable
540 phase separated domains. *eLife* **10**, doi:10.7554/eLife.64563 (2021).

541 66 Eeftens, J. M., Kapoor, M., Michieletto, D. & Brangwynne, C. P. Polycomb condensates can
542 promote epigenetic marks but are not required for sustained chromatin compaction. *Nature*
543 *Communications* **12**, 5888, doi:10.1038/s41467-021-26147-5 (2021).

544 67 Tatavosian, R. *et al.* Nuclear condensates of the Polycomb protein chromobox 2 (CBX2)
545 assemble through phase separation. *J Biol Chem* **294**, 1451-1463,
546 doi:10.1074/jbc.RA118.006620 (2019).

547 68 Boija, A. *et al.* Transcription factors activate genes through the phase-separation capacity of
548 their activation domains. *Cell* **175**, 1842-1855 e1816, doi:10.1016/j.cell.2018.10.042 (2018).

549 69 Hnisz, D., Shrinivas, K., Young, R. A., Chakraborty, A. K. & Sharp, P. A. A phase separation
550 model for transcriptional control. *Cell* **169**, 13-23, doi:10.1016/j.cell.2017.02.007 (2017).

551 70 Shrinivas, K. *et al.* Enhancer features that drive formation of transcriptional condensates.
552 *Molecular Cell* **75**, 549-561 (2019).

553 71 Cho, W. K. *et al.* Mediator and RNA polymerase II clusters associate in transcription-
554 dependent condensates. *Science* **361**, 412-415, doi:10.1126/science.aar4199 (2018).

555 72 Sabari, B. R. *et al.* Coactivator condensation at super-enhancers links phase separation and
556 gene control. *Science* **361**, eaar3958, doi:10.1126/science.aar3958 (2018).

557 73 Mansour, M. R. *et al.* Oncogene regulation. An oncogenic super-enhancer formed through
558 somatic mutation of a noncoding intergenic element. *Science* **346**, 1373-1377,
559 doi:10.1126/science.1259037 (2014).

560 74 Reiter, F., Wienerroither, S. & Stark, A. Combinatorial function of transcription factors and
561 cofactors. *Curr Opin Genet Dev* **43**, 73-81, doi:10.1016/j.gde.2016.12.007 (2017).

562 75 Sorrells, T. R., Booth, L. N., Tuch, B. B. & Johnson, A. D. Intersecting transcription networks
563 constrain gene regulatory evolution. *Nature* **523**, 361-365, doi:10.1038/nature14613 (2015).

564 76 Beyhan, S., Gutierrez, M., Voorhies, M. & Sil, A. A temperature-responsive network links cell
565 shape and virulence traits in a primary fungal pathogen. *PLoS Biol* **11**, e1001614,
566 doi:10.1371/journal.pbio.1001614 (2013).

567 77 Borneman, A. R. *et al.* Divergence of transcription factor binding sites across related yeast
568 species. *Science* **317**, 815-819 (2007).

569 78 Nobile, C. J. *et al.* A recently evolved transcriptional network controls biofilm development in
570 *Candida albicans*. *Cell* **148**, 126-138, doi:S0092-8674(11)01361-4 [pii]
571 10.1016/j.cell.2011.10.048 (2012).

572 79 Gomez-Pastor, R., Burchfiel, E. T. & Thiele, D. J. Regulation of heat shock transcription
573 factors and their roles in physiology and disease. *Nature Reviews. Molecular Cell Biology* **19**,
574 4-19, doi:10.1038/nrm.2017.73 (2018).

575 80 Hernday, A. D. *et al.* Structure of the transcriptional network controlling white-opaque
576 switching in *Candida albicans*. *Mol Microbiol* **90**, 22-35, doi:10.1111/mmi.12329 (2013).

577 81 Zordan, R. E., Miller, M. G., Galgoczy, D. J., Tuch, B. B. & Johnson, A. D. Interlocking
578 transcriptional feedback loops control white-opaque switching in *Candida albicans*. *PLoS Biol*
579 **5**, e256 (2007).

580 82 Frazer, C. *et al.* Epigenetic cell fate in *Candida albicans* is controlled by transcription factor
581 condensates acting at super-enhancer-like elements. *Nat Microbiol*, doi:10.1038/s41564-020-
582 0760-7 (2020).

583 83 Chowdhary, S., Kainth, A. S., Pincus, D. & Gross, D. S. Heat shock factor 1 drives intergenic
584 association of its target gene loci upon heat shock. *Cell Reports* **26**, 18-28 e15,
585 doi:10.1016/j.celrep.2018.12.034 (2019).

586 84 Kainth, A. S., Chowdhary, S., Pincus, D. & Gross, D. S. Primordial super-enhancers: heat
587 shock-induced chromatin organization in yeast. *Trends Cell Biol* **31**, 801-813,
588 doi:10.1016/j.tcb.2021.04.004 (2021).

589 85 McSwiggen, D. T. *et al.* Evidence for DNA-mediated nuclear compartmentalization distinct
590 from phase separation. *eLife* **8**, doi:10.7554/eLife.47098 (2019).

591 86 Blobel, G. A., Higgs, D. R., Mitchell, J. A., Notani, D. & Young, R. A. Testing the super-
592 enhancer concept. *Nat Rev Genet* **22**, 749-755, doi:10.1038/s41576-021-00398-w (2021).

593 87 Chong, S. *et al.* Tuning levels of low-complexity domain interactions to modulate endogenous
594 oncogenic transcription. *Mol Cell*, doi:10.1016/j.molcel.2022.04.007 (2022).

595 88 Boehning, M. *et al.* RNA polymerase II clustering through carboxy-terminal domain phase
596 separation. *Nature Structural & Molecular Biology* **25**, 833-840, doi:10.1038/s41594-018-
597 0112-y (2018).

598 89 Lu, H. *et al.* Phase-separation mechanism for C-terminal hyperphosphorylation of RNA
599 polymerase II. *Nature* **558**, 318-323, doi:10.1038/s41586-018-0174-3 (2018).

600 90 Burke, K. A., Janke, A. M., Rhine, C. L. & Fawzi, N. L. Residue-by-residue view of *in vitro*
601 FUS granules that bind the C-terminal domain of RNA polymerase II. *Mol Cell* **60**, 231-241,
602 doi:10.1016/j.molcel.2015.09.006 (2015).

603 91 Guo, Y. E. *et al.* Pol II phosphorylation regulates a switch between transcriptional and splicing
604 condensates. *Nature* **572**, 543-548, doi:10.1038/s41586-019-1464-0 (2019).

605 92 Portz, B. & Shorter, J. Switching condensates: The CTD code goes liquid. *Trends Biochem Sci*
606 **45**, 1-3, doi:10.1016/j.tibs.2019.10.009 (2020).

607 93 Quintero-Cadena, P., Lenstra, T. L. & Sternberg, P. W. RNA Pol II length and disorder enable
608 cooperative scaling of transcriptional bursting. *Mol Cell* **79**, 207-220 e208,
609 doi:10.1016/j.molcel.2020.05.030 (2020).

610 94 Henninger, J. E. *et al.* RNA-mediated feedback control of transcriptional condensates. *Cell* **184**,
611 207-225 e224, doi:10.1016/j.cell.2020.11.030 (2021).

612 95 Shao, W. *et al.* Phase separation of RNA-binding protein promotes polymerase binding and
613 transcription. *Nature Chemical Biology* **18**, 70-80, doi:10.1038/s41589-021-00904-5 (2022).

614 96 Bi, X. *et al.* RNA targets ribogenesis factor WDR43 to chromatin for transcription and
615 pluripotency control. *Mol Cell* **75**, 102-116 e109, doi:10.1016/j.molcel.2019.05.007 (2019).

616 97 Chen, G. *et al.* Taf14 recognizes a common motif in transcriptional machineries and facilitates
617 their clustering by phase separation. *Nature Communications* **11**, 4206, doi:10.1038/s41467-
618 020-18021-7 (2020).

619 98 Rencus-Lazar, S., DeRowe, Y., Adsi, H., Gazit, E. & Laor, D. Yeast models for the study of
620 amyloid-associated disorders and development of future therapy. *Front Mol Biosci* **6**, 15,
621 doi:10.3389/fmolsb.2019.00015 (2019).

622 99 Tuite, M. F. Yeast models of neurodegenerative diseases. *Prog Mol Biol Transl Sci* **168**, 351-
623 379, doi:10.1016/bs.pmbts.2019.07.001 (2019).

624 100 Zbinden, A., Perez-Berlanga, M., De Rossi, P. & Polymenidou, M. Phase separation and
625 neurodegenerative diseases: A disturbance in the force. *Dev Cell* **55**, 45-68,
626 doi:10.1016/j.devcel.2020.09.014 (2020).

627 101 Darling, A. L. & Shorter, J. Combating deleterious phase transitions in neurodegenerative
628 disease. *Biochim Biophys Acta Mol Cell Res* **1868**, 118984, doi:10.1016/j.bbamcr.2021.118984
629 (2021).

630 102 Sun, Z. *et al.* Molecular determinants and genetic modifiers of aggregation and toxicity for the
631 ALS disease protein FUS/TLS. *PLoS Biol* **9**, e1000614, doi:10.1371/journal.pbio.1000614
632 (2011).

633 103 Elden, A. C. *et al.* Ataxin-2 intermediate-length polyglutamine expansions are associated with
634 increased risk for ALS. *Nature* **466**, 1069-1075, doi:10.1038/nature09320 (2010).

635 104 Shorter, J. Designer protein disaggregases to counter neurodegenerative disease. *Curr Opin
636 Genet Dev* **44**, 1-8, doi:10.1016/j.gde.2017.01.008 (2017).

637 105 Tariq, A. *et al.* Mining disaggregase sequence space to safely counter TDP-43, FUS, and alpha-
638 synuclein proteotoxicity. *Cell Reports* **28**, 2080-2095 e2086, doi:10.1016/j.celrep.2019.07.069
639 (2019).

640 106 Oldfield, C. J. & Dunker, A. K. Intrinsically disordered proteins and intrinsically disordered
641 protein regions. *Annu Rev Biochem* **83**, 553-584, doi:10.1146/annurev-biochem-072711-
642 164947 (2014).

643 107 Martin, E. W. *et al.* Valence and patterning of aromatic residues determine the phase behavior
644 of prion-like domains. *Science* **367**, 694-699, doi:10.1126/science.aaw8653 (2020).

645 108 Pak, C. W. *et al.* Sequence determinants of intracellular phase separation by complex
646 coacervation of a disordered protein. *Mol Cell* **63**, 72-85, doi:10.1016/j.molcel.2016.05.042
647 (2016).

648 109 Bremer, A. *et al.* Deciphering how naturally occurring sequence features impact the phase
649 behaviours of disordered prion-like domains. *Nat Chem* **14**, 196-207, doi:10.1038/s41557-021-
650 00840-w (2022).

651 110 Wang, J. *et al.* A molecular grammar governing the driving forces for phase separation of
652 prion-like RNA binding proteins. *Cell* **174**, 688-699 e616, doi:10.1016/j.cell.2018.06.006
653 (2018).

654 111 Vernon, R. M. *et al.* Pi-Pi contacts are an overlooked protein feature relevant to phase
655 separation. *eLife* **7**, doi:10.7554/eLife.31486 (2018).

656 112 Lin, Y., Currie, S. L. & Rosen, M. K. Intrinsically disordered sequences enable modulation of
657 protein phase separation through distributed tyrosine motifs. *J Biol Chem* **292**, 19110-19120,
658 doi:10.1074/jbc.M117.800466 (2017).

659 113 Murthy, A. C. *et al.* Molecular interactions underlying liquid-liquid phase separation of the
660 FUS low-complexity domain. *Nature Structural & Molecular Biology* **26**, 637-648,
661 doi:10.1038/s41594-019-0250-x (2019).

662 114 Conicella, A. E. *et al.* TDP-43 alpha-helical structure tunes liquid-liquid phase separation and
663 function. *Proc Natl Acad Sci U S A* **117**, 5883-5894, doi:10.1073/pnas.1912055117 (2020).

664 115 Conicella, A. E., Zerze, G. H., Mittal, J. & Fawzi, N. L. ALS mutations disrupt phase
665 separation mediated by alpha-helical structure in the TDP-43 low-complexity C-terminal
666 domain. *Structure* **24**, 1537-1549, doi:10.1016/j.str.2016.07.007 (2016).

667 116 Murray, D. T. *et al.* Structure of FUS protein fibrils and its relevance to self-assembly and
668 phase separation of low-complexity domains. *Cell* **171**, 615-627 e616,
669 doi:10.1016/j.cell.2017.08.048 (2017).

670 117 Kato, M. *et al.* Cell-free formation of RNA granules: low complexity sequence domains form
671 dynamic fibers within hydrogels. *Cell* **149**, 753-767, doi:10.1016/j.cell.2012.04.017 (2012).

672 118 Kato, M., Zhou, X. & McKnight, S. L. How do protein domains of low sequence complexity
673 work? *RNA* **28**, 3-15, doi:10.1261/rna.078990.121 (2022).

674 119 Fawzi, N. L., Parekh, S. H. & Mittal, J. Biophysical studies of phase separation integrating
675 experimental and computational methods. *Current Opinion in Structural Biology* **70**, 78-86,
676 doi:10.1016/j.sbi.2021.04.004 (2021).

677 120 Banani, S. F., Lee, H. O., Hyman, A. A. & Rosen, M. K. Biomolecular condensates: organizers
678 of cellular biochemistry. *Nature Reviews. Molecular Cell Biology* **18**, 285-298,
679 doi:10.1038/nrm.2017.7 (2017).

680 121 Banani, S. F. *et al.* Compositional control of phase-separated cellular bodies. *Cell* **166**, 651-
681 663, doi:10.1016/j.cell.2016.06.010 (2016).

682 122 Mittag, T. & Pappu, R. V. A conceptual framework for understanding phase separation and
683 addressing open questions and challenges. *Mol Cell* **82**, 2201-2214,
684 doi:10.1016/j.molcel.2022.05.018 (2022).

685 123 Brangwynne, C. P. Phase transitions and size scaling of membrane-less organelles. *J Cell Biol*
686 **203**, 875-881, doi:10.1083/jcb.201308087 (2013).

687 124 Dutagaci, B. *et al.* Charge-driven condensation of RNA and proteins suggests broad role of
688 phase separation in cytoplasmic environments. *eLife* **10**, doi:10.7554/eLife.64004 (2021).

689 125 Dignon, G. L., Best, R. B. & Mittal, J. Biomolecular phase separation: From molecular driving
690 forces to macroscopic properties. *Annu Rev Phys Chem* **71**, 53-75, doi:10.1146/annurev-
691 physchem-071819-113553 (2020).

692 126 Garcia-Jove Navarro, M. *et al.* RNA is a critical element for the sizing and the composition of
693 phase-separated RNA-protein condensates. *Nature Communications* **10**, 3230,
694 doi:10.1038/s41467-019-11241-6 (2019).

695 127 Guillen-Boixet, J. *et al.* RNA-induced conformational switching and clustering of G3BP drive
696 stress granule assembly by condensation. *Cell* **181**, 346-361 e317,
697 doi:10.1016/j.cell.2020.03.049 (2020).

698 128 Maharana, S. *et al.* RNA buffers the phase separation behavior of prion-like RNA binding
699 proteins. *Science* **360**, 918-921, doi:10.1126/science.aar7366 (2018).

700 129 Ma, W., Zheng, G., Xie, W. & Mayr, C. *In vivo* reconstitution finds multivalent RNA-RNA
701 interactions as drivers of mesh-like condensates. *eLife* **10**, doi:10.7554/eLife.64252 (2021).

Super-enhancer features	Mammalian super-enhancers	<i>C. albicans</i> super-enhancer-like regions
Role in cell identity	Found to control cell identity and differentiation in murine embryonic stem cells (ESCs), multiple immune cell type, and to contribute to a broad range of cancers via enrichment at genes with oncogenic function.	Extended regulatory regions are required for white-opaque cell fate determination and additionally for control of biofilm formation, whereby cells transition between planktonic growth and communal growth.
	Median size is > 8 kb, whereas typical enhancers are ~700 bp.	For the white-opaque TRN, median size of upstream intergenic regions is > 7 kb, while average intergenic regions are ~ 557 bp.
TF enrichment levels	Elevated TF binding at constituent enhancers, increased cooperative transcriptional activation, and combined TF/coactivator enrichment ~10-fold higher than seen at typical enhancers.	Master TFs bind together at multiple positions across super-enhancer-like regions (see Fig. 5), although quantitative analysis of cofactor levels has not been performed.
Epigenetic marks	Relatively high levels of acetylation of histone H3 at lysine 27 (H3K27ac) are commonly used to define super-enhancers, sometimes in combination with other criteria.	Unknown.
Sensitivity to TF perturbation	Highly sensitive – blocking binding of just one coactivator, like BRD4, can collapse entire super-enhancer.	Highly sensitive – a small increase or decrease in levels of the Wor1 TF, for example, can drastically alter white-opaque cell fate switching rates.

708 **Figure Legends**

709

710 **Figure 1. Stress granule and P body formation in response to environmental changes.**

711 Extracellular stress such as heat shock or a sudden drop in pH leads to global inhibition of translation
712 and ribosome stalling. Stalled mRNAs are diverted to either P bodies or stress granules. Following
713 pH stress, stress granules dissolve spontaneously, whereas stress granules formed following
714 temperature stress require the assistance of Hsp40, Hsp70 and Hsp104. Subsets of mRNAs that are
715 concentrated in P bodies can either be degraded or exchanged with stress granules.

716

717 **Figure 2. The effect of molecular crowding on phase separation.**

718 **a**, Microrheology using self-assembling Genetically Encoded Multimers (GEMs) allows measurement
719 of intracellular crowding in the nucleus and the cytoplasm. Individual monomers consist of a
720 *Pyrococcus furiosus* encapsulin scaffold fused to a fluorescent protein and spontaneously assemble
721 into 40 nm spheres. The nucleus is a more crowded milieu than the cytoplasm and thus the random
722 thermal motion of GEMs is decreased. **b**, mTORC activation following starvation results in an
723 increased ribosome number. This increase in molecular crowding can increase phase separation of
724 cytoplasmic proteins. Adapted from ³⁰.

725

726 **Figure 3. Phase separation in polarized growth, cell asymmetry and nuclear divisions.**

727 **a**, Spa2 localizes Aip5 to the *S. cerevisiae* bud tip, recruiting Bni1 and nucleating actin filaments.
728 Stresses such as low pH or energy depletion result in Aip5 and Spa5 forming cytoplasmic condensates.
729 When both Aip5 and Spa2 are present, these condensates are rapidly disassembled following removal
730 of the stress. In the absence of Spa2, Aip5 forms more stable condensates that are not readily
731 disassembled and there is a consequent loss of viability following prolonged stress. Adapted from ³⁴.
732 **b**, In *A. gossypii*, mRNA binding protein Whi3 forms distinct protein/mRNA condensates. Whi3

733 condensates formed with Bni1 and Spa2 mRNA are localized to the site of branch formation (symmetry
734 breaking) where they nucleate actin assembly. Whi3 droplets containing Cln3 mRNA form adjacent to
735 the nucleus where they regulate asynchronous nuclear division (cell cycle regulation). Adapted from ³⁶.

736

737 **Figure 4. Phase separation regulation of bulk and selective autophagy.**

738 **a**, When nutrients are abundant, Atg13 is hyperphosphorylated by TORC1 kinase. Upon nutrient
739 starvation, Atg13 is dephosphorylated by PP2C phosphatase enabling interactions with the Atg17-29-
740 31 complex and the Atg1 kinase which then coalesce into condensates. The resulting Pre-
741 Autophagosomal Structure (PAS) is tethered to the vacuolar membrane by interactions with Vac8. In
742 the newly formed PAS, Atg1 auto-phosphorylates itself and hyper-phosphorylates Atg13.

743 Cytoplasmic phospho-Atg13 is trafficked back to the PAS following dephosphorylation by PP2C.

744 Thus, Atg1 and PP2C maintain an equilibrium of unphosphorylated and phosphorylated Atg13 which
745 maintains the PAS. The PAS is also the site of Isolation Membrane formation, which in turn will
746 become the mature autophagosome. **Inset**, Following PAS formation, vacuoles containing ATG9 are
747 recruited and subsequently fuse to become the cupped isolation membrane, which grows to engulf
748 materials destined for destruction in the lysosome. **b**, Dodecamers of Ape1 undergo phase separation
749 and are degraded by selective autophagy in nutrient rich conditions. The Ape1 condensate is coated by
750 a shell of the Atg9 adapter protein which templates growth of Atg8-decorated isolation membrane.

751 Ape1 mutants which form aggregates are not engulfed. Adapted from ⁴⁷.

752

753 **Figure 5. Phase separation regulates transcription and fungal cell fate.**

754 **a**, Coordinated binding of multiple TFs to regions upstream of their ORFs is often observed even
755 without consensus binding sites for these regulators, suggestive of recruitment by protein-protein
756 interactions. **b**, A phase separation model of transcription where TFs form condensates together with
757 the transcriptional machinery to regulate the expression of cell identity genes. **c**, *C. albicans* switches

758 epigenetically between “white” and “opaque” phenotypic states. **d**, The white-to-opaque transition is
759 regulated by a TF network whose members bind to their own promoters as well as those of others in
760 the network, as indicated by the arrows. Adapted from ref⁸². **e**, RNA polymerase II interacts with
761 transcriptional initiation or elongation condensates depending on the phosphorylation state of its C-
762 terminal domain (CTD).

763

764 **Box 1. Molecular forces promoting phase separation**

765 Multivalent interactions, in which a single component contacts multiple other components, are
766 critical drivers of phase separation. Multivalency can be achieved by proteins with intrinsically
767 disordered regions (IDRs) or can involve interactions between folded domains and short linear motifs
768 (SLiMs) that are sequence-specific recognition sites^{1,3,106-109}. Prion-like domains (PrLDs) are a
769 particularly important class of IDRs and are defined by their sequence composition which is enriched
770 in uncharged polar amino acids and glycine similar to *S. cerevisiae* prions.

771 A “sticker and spacer” model has been developed to describe how phase-separating IDRs
772 interact. This simplified model defines “sticker” residues as those involved in electrostatic,
773 hydrophobic, cation–Pi or Pi–Pi interactions, while “spacer” residues do not contribute to
774 intermolecular interactions^{109,110}. Attention has focused on aromatic residues as important “stickers”
775 that can form Pi–Pi interactions with other aromatic residues or cation–Pi interactions with basic
776 residues^{107,109-111}. The nature of the spacer residues also defines biocondensate properties with glycine
777 spacers promoting liquid behavior whereas glutamine/serine spacers promote solidifying of
778 condensates¹¹⁰.

779 Overall, many residue types and intermolecular forces can contribute to phase separation, such
780 as hydrophobic contacts/amino acids that can drive condensation of IDRs^{108,112,113}. Formation of
781 transient structures (including β-sheets and intermolecular helical regions) can also increase self-

782 assembly and condensation formation¹¹⁴⁻¹¹⁶. In fact, one model proposes that transient structures are
783 intermediate events in the formation of labile β -sheet structures that drive LLPS¹¹⁶⁻¹¹⁸, although this
784 model is contested^{113,119}.

785 Phase-separating molecules have further been designated as “scaffolds”, that are both necessary
786 and sufficient for phase separation, and “clients”, which can selectively partition into condensates but
787 do not phase separate by themselves^{120,121}. Condensation also can be coupled to the formation of a
788 system-spanning or “percolation” interaction network, although percolation networks can also occur
789 independently of phase separation¹²².

790

791 **Box 1 Fig Legend. Weak protein-protein interactions and multivalency drive phase separation.**

792 **a**, Phase separation occurs when protein concentration, osmolarity, temperature, and/or pH cross a
793 threshold where intermolecular interactions drive assembly into a dense phase that co-exists with the
794 surrounding dilute phase (adapted from ref¹²³). **b**, Higher valency due to a higher number of potential
795 interactions between two peptide chains promotes phase separation. **c**, A “sticker” and “spacer” model
796 for phase separation. Charged and aromatic “sticker” residues (larger balls) are distributed along a
797 polypeptide interspersed with stretches of polar, hydrophilic residues (smaller balls) that act as
798 “spacer” residues. **d**, “Scaffold” proteins have the capacity to undergo phase separation independent of
799 other factors due to their high valency. Scaffolds can recruit “client” proteins that by themselves are
800 not able to undergo phase separation under the same conditions.

801

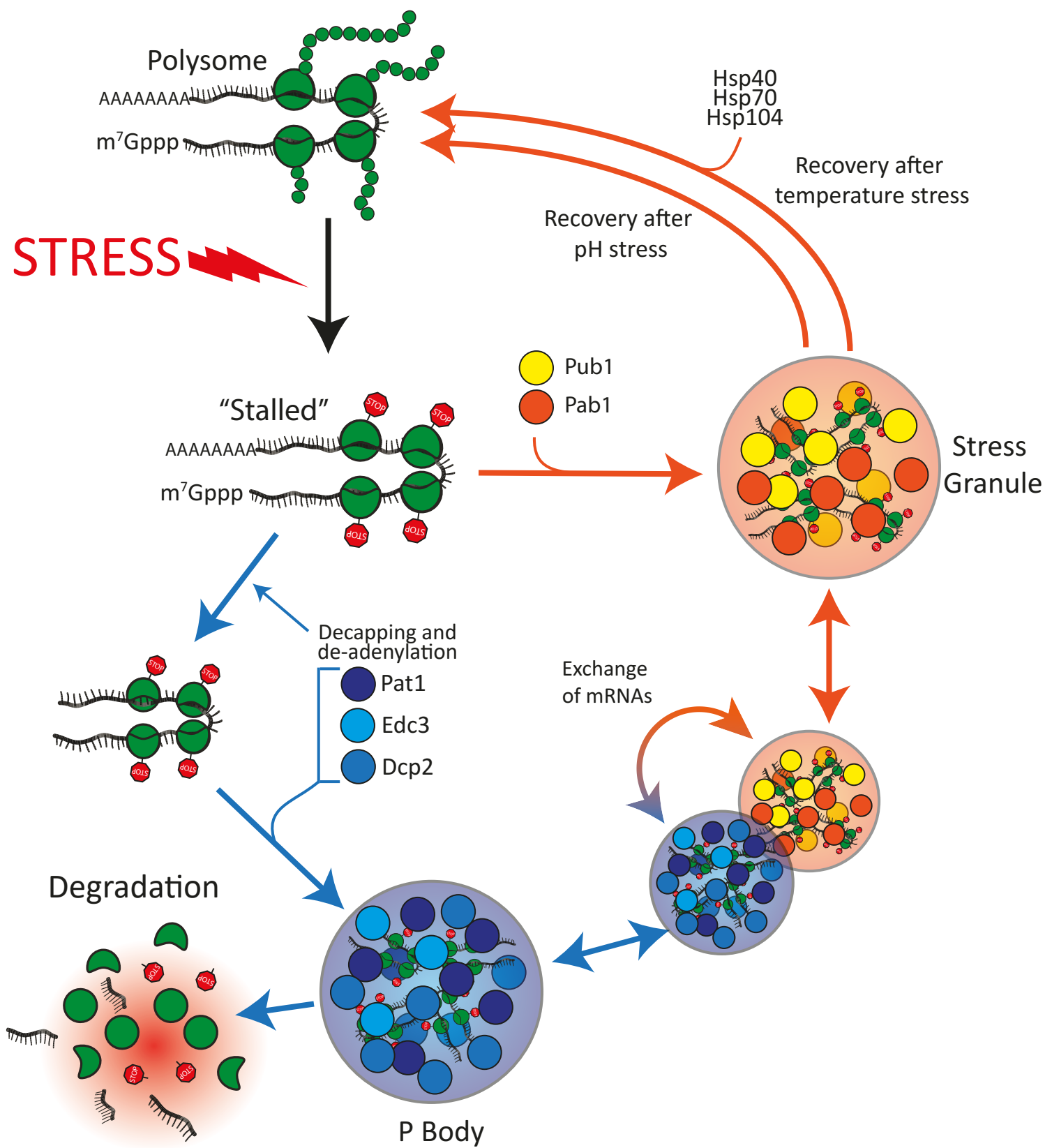
802 **Box 2. Protein-nucleic acid interactions drive condensate formation**

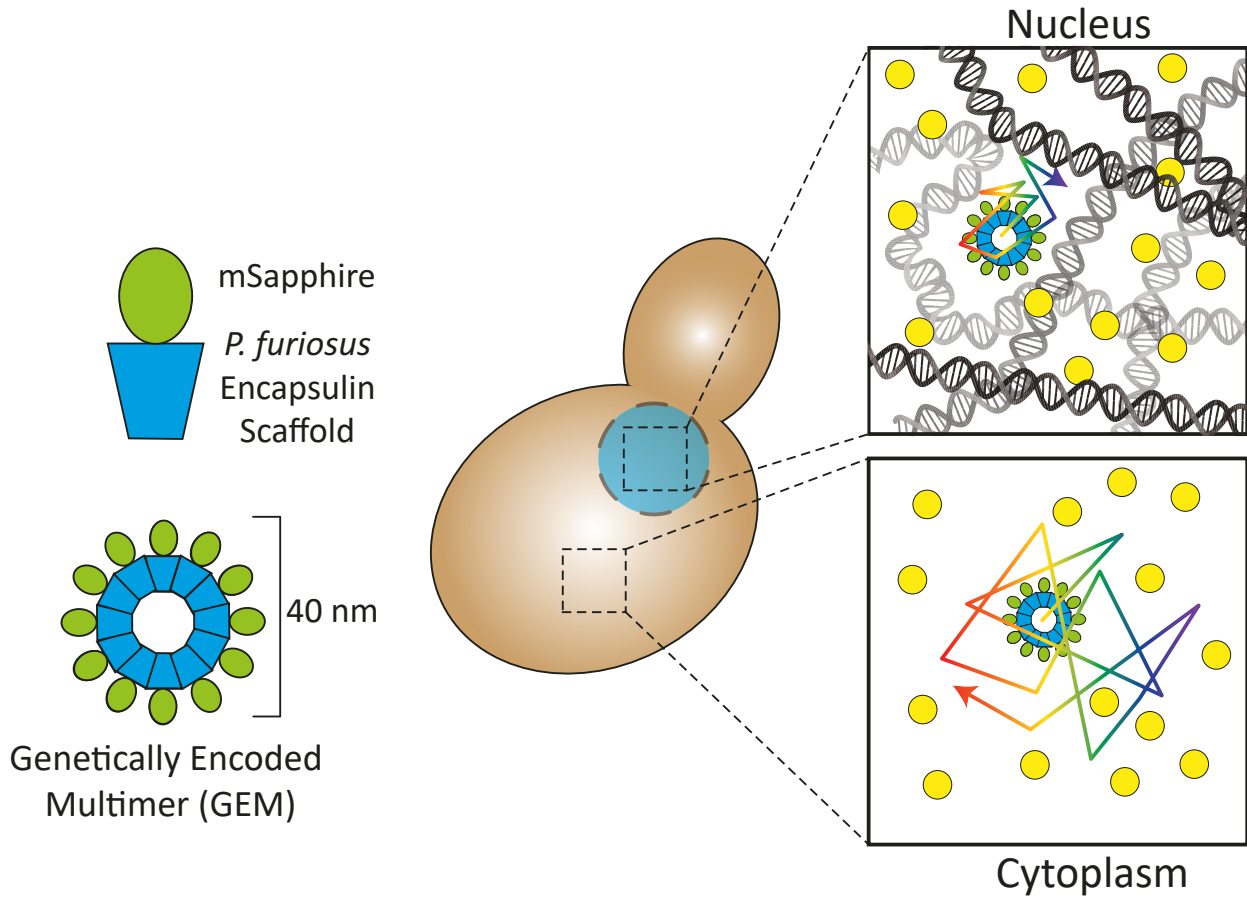
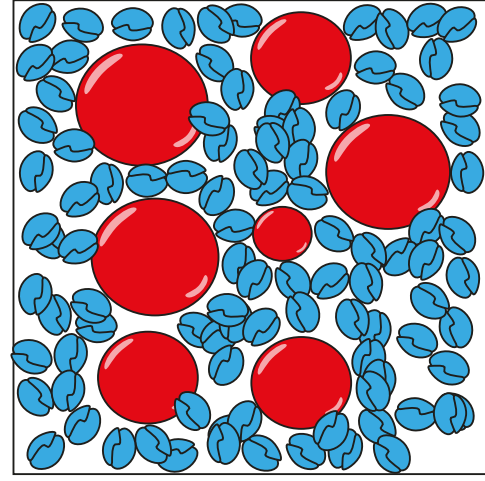
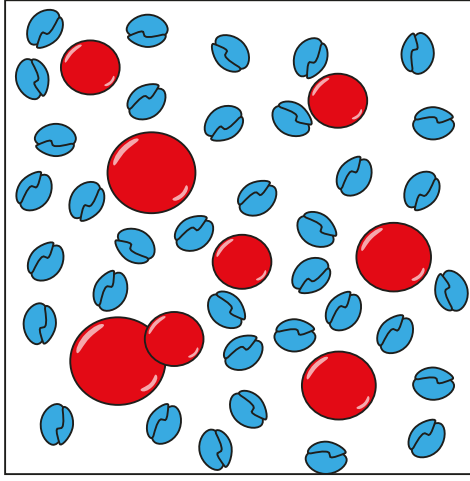
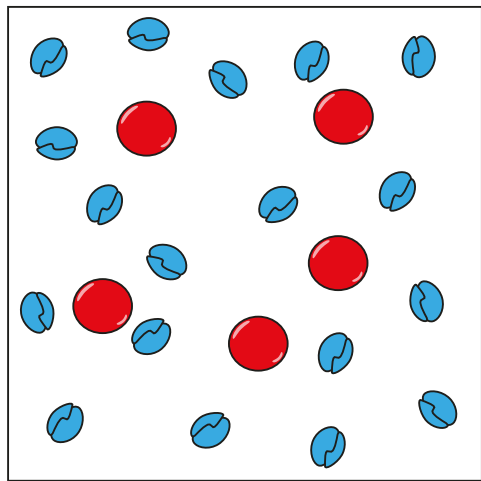
803 Negatively charged nucleic acids can interact with positively charged proteins to drive phase
804 separation, a form of complex coacervation where multivalent nucleic acid-binding domains can
805 support condensate formation even in the absence of IDRs¹²⁴. Single-stranded nucleic acids can also
806 participate in cation-pi or pi-pi interactions through exposed aromatic bases thereby supporting

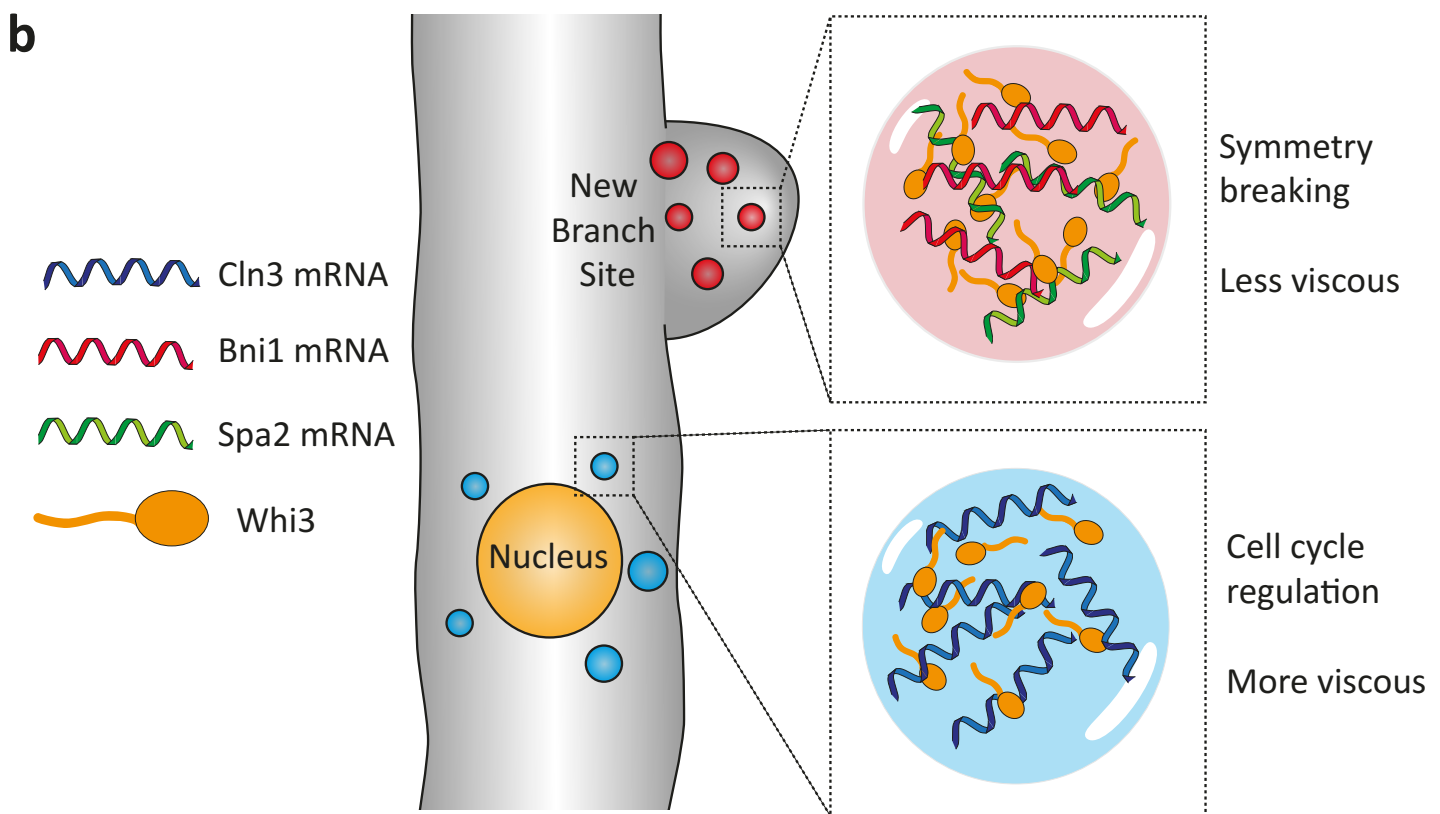
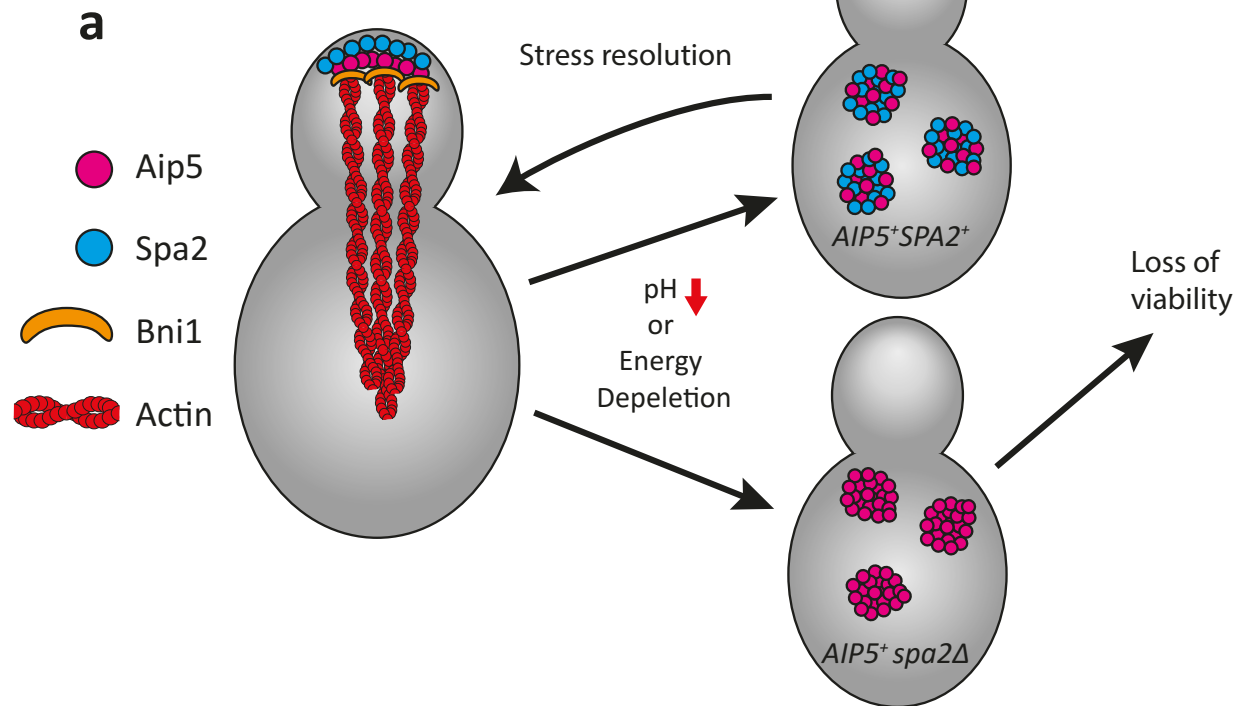
807 condensate formation, while recognition of nucleotide bases via hydrogen bonds is an additional
808 driving force for phase separation¹²⁵.

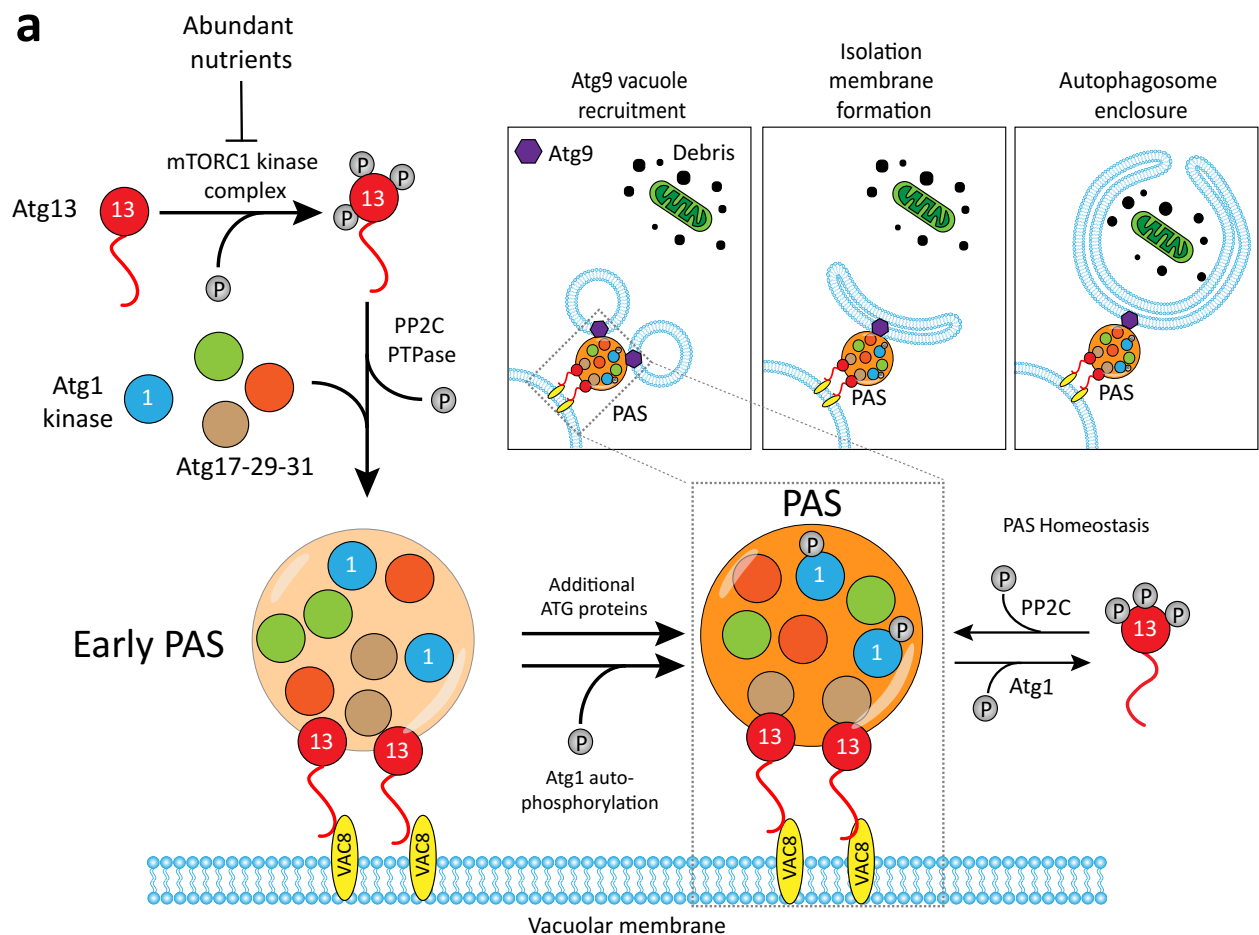
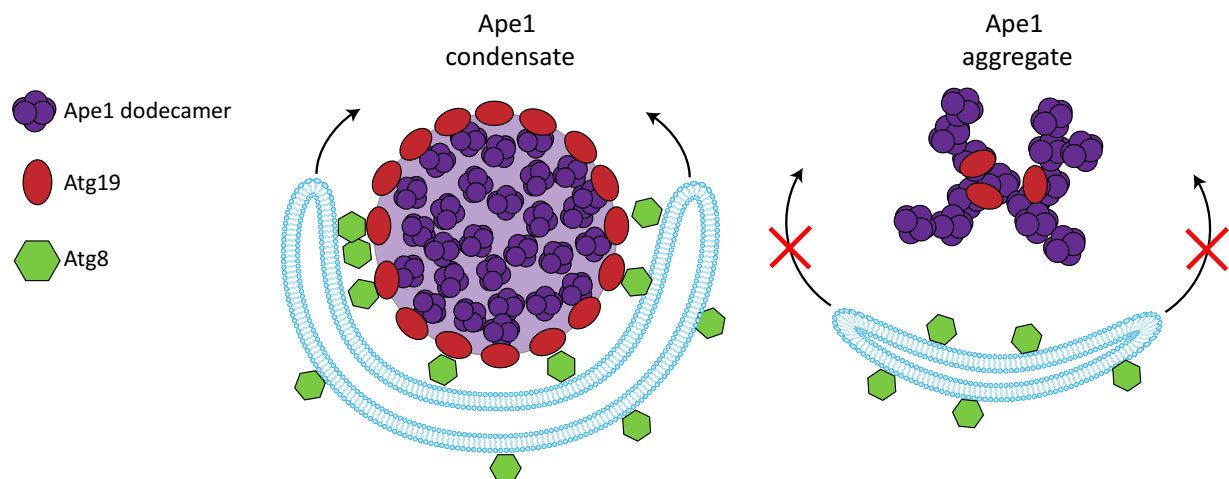
809 RNA is a critical component of multiple condensates including stress granules, storage
810 granules, and various speckles, paraspeckles, nuclear speckles and transcriptional complexes. RNA
811 transcripts can directly seed the nucleation of condensates or can induce protein conformations that
812 promote condensation^{126,127}. RNA levels can also tune phase separation of ribonucleoprotein (RNP)
813 condensates. For example, low RNA levels stimulate condensate formation by human FUS protein
814 while high RNA levels suppress condensate formation, and changes in RNA concentrations may
815 underlie aberrant LLPS structures and pathologic assemblies¹²⁸. While liquid condensates adopt a
816 spherical shape in the absence of external forces, certain RNP-containing condensates form highly
817 viscous structures, mesh-like assemblies or filamentous networks depending on the RNA substrates
818 involved, highlighting how various shapes and structures can arise via phase separation^{39,129}.

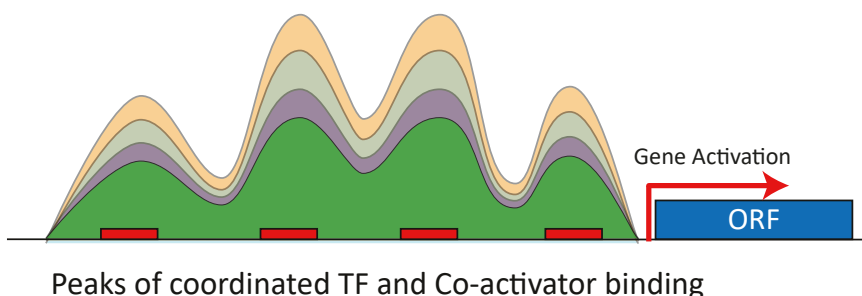
819



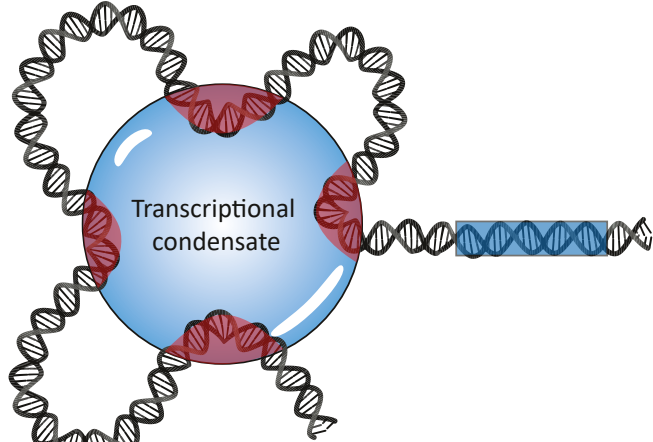
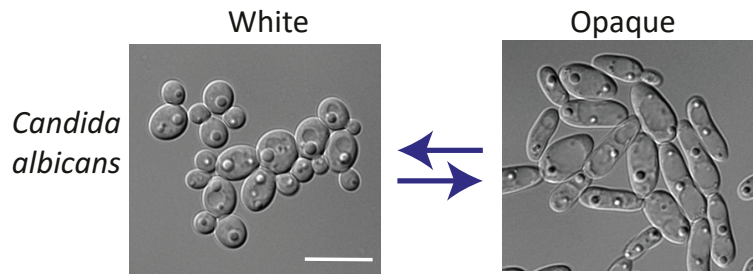
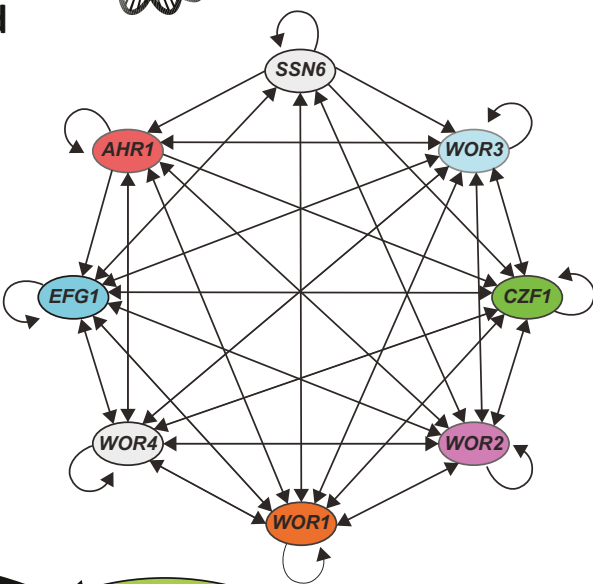
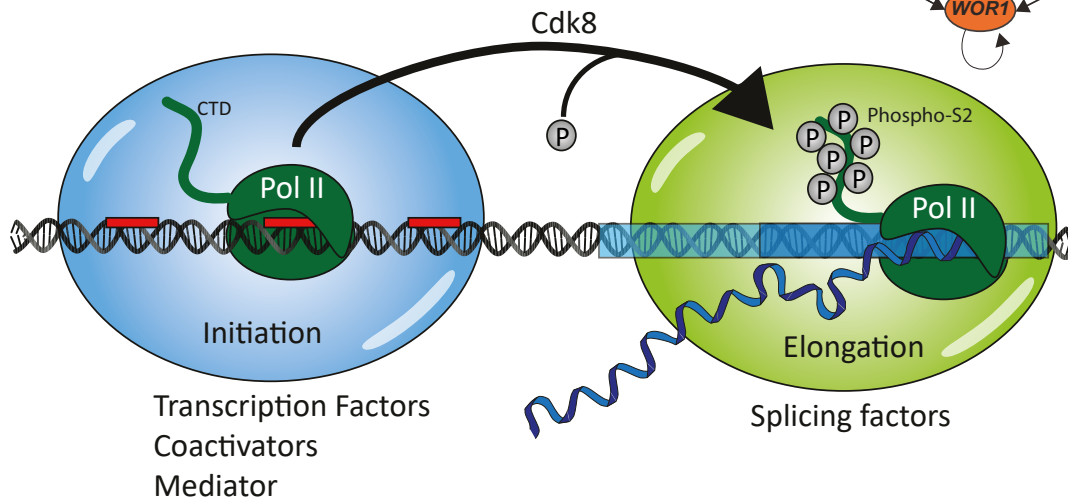
a**b****mTORC1****Ribosomes** (blue circles)**Phase Separation** (red circle)

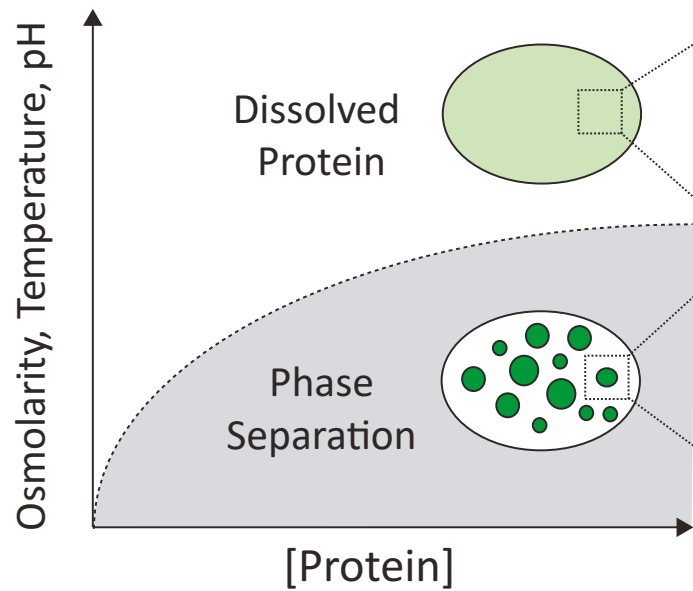
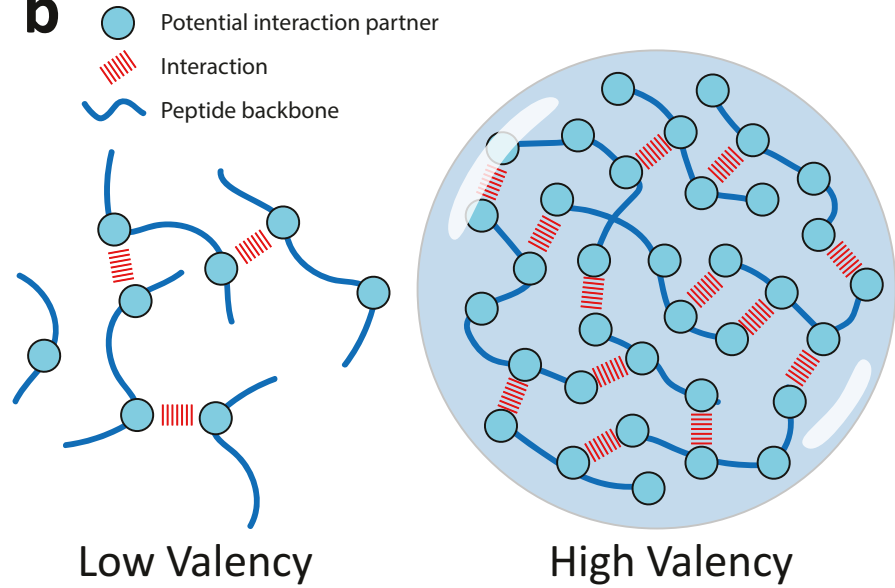
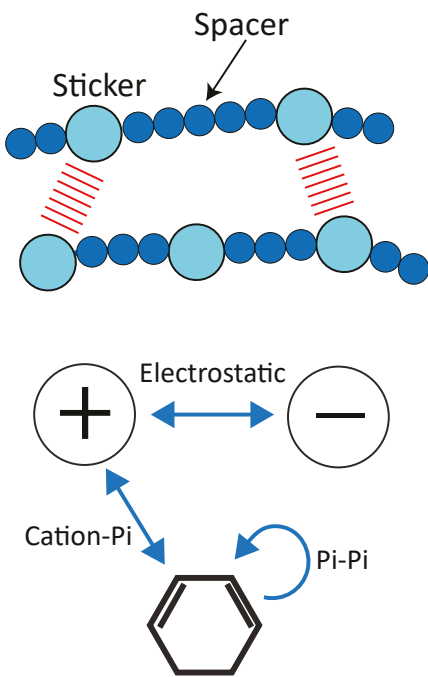


a**b**

a

Peaks of coordinated TF and Co-activator binding

b**c****d****e**

a**b****c****d**